Journal of Computer Science & Computational Mathematics, Volume 8, Issue 4, December 2018
DOI: 10.20967/jcscm.2018.04.009

Numerical Assessment of Anisotropic Diffusion Equation for Image Blurring Using SOR Iteration

Nurul Afiqah Basran[1*], Jeng Hong Eng[1], Azali Saudi[2], Jumat Sulaiman[1]

[1]Faculty of Science and Natural Resources, Universiti Malaysia Sabah
[2]Knowledge Technology Research Unit, Faculty of Computing and Informatics, Universiti Malaysia Sabah, Kota Kinabalu, Malaysia
[*]Corresponding author email: nurulafiqahbasran@yahoo.com

***Abstract*:** Blurring the image while preserving the important features such as edges is a crucial study in computer vision. This paper presents the results of applying three iterative methods which are Jacobi, Gauss Seidel and Successive Overrelaxation (SOR) to solve anisotropic diffusion equation for image blurring, where the output image of Jacobi is used as a control image. The number of iterations and computational time required to solve the anisotropic diffusion equation are used to measure the performance of the considered iterative methods. The findings show that SOR method is more efficient to smooth the inner region of an image compared to Jacobi and Gauss-Seidel methods in which the SOR required the least number of iterations and computational time.

***Keywords*:** diffusion equation, partial difference equation, image blurring, SOR method.

1. Introduction

The application of mathematical models in image processing and analysis has begun since early 1960 [1], where the field was highly occupied in study of computer science and engineering. Numerical method is one of the mathematical tools used to solve image processing problems especially using techniques of functional analysis and the theory of partial differential equations (PDEs). Nowadays, many researchers employ the diffusion-wave equation [2], heat equation [3], Poisson Equation [4] and Laplace equation as PDE-based image processing techniques for image segmentation [5], image restoration-denoising and deblurring[6], edge detection and enhancement [7] purposes. In image processing, image blurring is also known as the process of image denoising, smoothing or edge detection.

The finite difference method (FDM) has been applied for the solution of PDEs by approximating any partial derivatives. There are three standard types of PDEs that consist of elliptic, hyperbolic and parabolic. The two-dimensional heat or diffusion equation applied on image blurring techniques is one of parabolic PDEs [8]. The approximation equations derived after discretization process can be made by using explicit, implicit, Crank-Nicholson or other schemes. The solution of the generated system of linear equations can be solved by using direct or iterative methods. Furthermore, diffusion or heat equation applied in image processing and analysis can also be referred as the scale space. The theory of scale space provided a framework to undergo various image processing techniques across multiple scales [9].

In this study, three iterative methods were applied to solve an anisotropic diffusion equation for image blurring. The approximate equation is derived using implicit scheme to discretize diffusion equation in which this approximation equation can be used to construct the generated system of linear equations. Then, this linear system can be solved iteratively by using Jacobi, Gauss-Seidel and SOR methods. In previous studies, it was proven that SOR method was the most suitable way to solve image blending problem [10].

2. Related Work

The PDEs techniques had been widely used in image processing problems and their techniques also have been used to construct the reliable and fast algorithm that is numerically efficient to solve the problem. Image processing problem based on diffusion equation or also known as the scale space had been discussed by Weickert *et al.* [9]. This equation has been widely applied for image filtering including image denoising, segmentation and edge detection. It has also been used in other fields of study such as biomedical by providing the important information from the image effectively. For example, the study conducted by Yilmaz *et al*. [11] applied an adaptive anisotropic diffusion to filter out unnecessary noise occurred on cone beam computed tomography (CBCT) images in order to identify the region of interest (ROI) in the diagnosis process.

An improved nonlinear diffusion algorithm had been developed [12] for image denoising problem. Noise is a random signal that appears as random speckles which significantly corrupt the image quality. Therefore, the new method had been verified as an efficient method to reduce image noise while maintaining important detail using wavelet coefficient. A recent study conducted [13] in image denoising problem, proved that a combination of classical additive operator splitting and a nonlinear relaxation algorithm are able to produce an accurate image restoration which is also able to control the problem of stability. Unlike the research conducted by Atlas *et al*. [14], more focusis on reducing the phenomenon of an image called staircase effect by proposing efficient tools through interpolation of two classical models which are Perona-Malik Equation (PME) and ρ −Laplacian with $\rho \rightarrow \infty$.

Meanwhile, the new diffusion coefficient has also been proposed [15] earlier for image smoothing method. They suggested a time-dependent anisotropic diffusion by investigating the relation between Gaussian scale and gradient

threshold with its stopping time based on an iterative signal-to-noise ration (SNR) measure. The accurate stopping time can avoid excessive smoothing that will disturb important edges and boundaries. Furthermore, the developed model also denoises the image faster than some traditional schemes such used in some studies [16, 17] while giving the highest value of normalized signal-to-noise ratio (NSNR).

Besides that, a recent study also had found the fastest way to denoises the image especially from the speckle noise that is present in medical imaging known as a Faster Oriented Speckle Reducing Anisotropic Diffusion filter (FOSRAD) method [18]. This method had successfully improved the execution time by optimizing the processing time using look-ahead decomposition technique. The result shows a significant decrease in execution time by 14X compared to original Oriented Speckle Reducing Anisotropic Diffusion (OSRAD) filter [19] which is more complex and also inappropriate for real time implementation.

Other than image denoising, diffusion equation also has been applied in solving the image segmentation problem. Segmentation of color image with Perona-Malik diffusion equation had been successfully discovered [20]. The pixels based technique of clustering applied to reduce unnecessary image details degrade the image quality throughout the homogeneous region and at the same time the boundaries between the region maintain sharp. The techniques are implemented by obtaining a histogram with the value of color pixels of an image and then are performed form a cluster based on the closest to the pixel color. The fuzzy k-mean clustering algorithm had been used and successfully produce segmented color images. Besides that, the same but more advanced algorithm which is the integration of Template based K-means and modified of Fuzzy C-means (TKFCM) clustering algorithm had efficiently used in brain MRI image to detect the tumor [21].

3. Anisotropic Diffusion Equation

The two-dimensional PDE techniques used for isotropic diffusion can be known as heat equation is given as follows:

$$\frac{\partial I}{\partial t} = \alpha\left(\frac{\partial^2 I}{\partial x^2} + \frac{\partial^2 I}{\partial y^2}\right) \quad , \; R \times [0,\infty) \tag{1}$$

Where the initial solution is given as $I(x,y,0) = f(x,y)$. Actually $f(x)$ is the experimental image with $\alpha = 1$. Solving equation (1) is equivalent to Gaussian smoothing by having the following solution [8]:

$$\frac{\partial I}{\partial t} = \begin{cases} f(x,y) & , \quad (t=0) \\ \left(G_{\sqrt{2t}} * f\right)(x,y) & , \quad (t>0) \end{cases} \tag{2}$$

where $G_\sigma(x)$ denotes as two-dimensional Gaussian filter known as:

$$G(x,y,\sigma) = \frac{1}{2\pi\sigma^2} e^{-\left(\frac{x^2+y^2}{2\sigma^2}\right)} \tag{3}$$

From equation (2), the time t and standard deviation of the Gaussian are related by $\sigma = \sqrt{2t}$. Hence, the convolution corresponds to a low-pass filtering and solved at different instance of time t and scale parameter σ of Gaussian Kernel.

An anisotropic diffusion is a technique used to remove the noise of the image by smoothing the inner region and at the same time preserves the edge information. The Perona-Malik model anisotropic diffusion equation is stated as [16]:

$$I_t = div(c(x,y,t)\nabla I \tag{4}$$

where div is a divergence operator and ∇I is a gradient magnitude operator respect to the spatial of x and y. Meanwhile, $c(x,y,t) = g(\|\nabla I(x,y,t)\|)$ is a diffusion coefficient used to control smoothing rate taken place at any location of an image (x,y). So the smoothing process will reduce the diffusivity in places with high possibilities to be the boundaries that can be controlled by using the local gradient magnitude function, $|\nabla I|$ where $c(x,y,t) = g(|\nabla I|)$. Then, the diffusion coefficient or edge stopping function $g(.)$ can be defined as [16]:

$$g(\nabla I) = e^{-\left(\frac{\|\nabla I\|}{K}\right)^2} \tag{5}$$

or

$$g(\nabla I) = \frac{1}{1+\left(\frac{\|\nabla I\|}{K}\right)^2}. \tag{6}$$

The small diffusion coefficient is applied at the location of the edges and at the larger $g(.)$ value for the inner region. The constant K in the function g is used to control the strength of the image edges in terms of gradient sensitivity [16]. Blurring effect with the small value of K is low, while using large value of K for $g(.)$ will result to low-pass filter in which the blurring effect on the image is high as $K \to \infty$ then let $\varepsilon = \frac{1}{K}$, it makes $\varepsilon \to 0$. In this research we used equation (6) as the edge stopping function.

3.1 Discretization of Anisotropic Diffusion Equation

Let the standard two-dimensional anisotropic diffusion equation used for image blurring problem in this study be given as follows:

$$\begin{cases} \frac{\partial I}{\partial t} = div(g(\|\nabla I\|)\nabla I) & ,R \times [0,\infty) \\ I(x,y,0) = f(x,y) & ,R \\ \langle g.\nabla I, n\rangle = 0 & ,\partial R \times [0,\infty) \end{cases} \tag{7}$$

with the Dirichlet boundary conditions. Then, the derivative in equation (7) can be discretized as shown below:

$$\frac{\partial I}{\partial t} = \frac{I_{i,j,k+1} - I_{i,j,k}}{\Delta t} \tag{8}$$

$$div(g(\|\nabla I\|)\nabla I) = \frac{\partial}{\partial x}(g.\nabla I_x)\Big|_{i,j,k+1} + \frac{\partial}{\partial y}(g.\nabla I_y)\Big|_{i,j,k+1} \tag{9}$$

Then, the approximations of equation (9) are used as follows:

$$\frac{\partial}{\partial x}(g.\nabla I_x)\Big|_{i,j,k+1} \approx \frac{g.I_x|_{i+\frac{1}{2},j,k+1} - g.I_x|_{i-\frac{1}{2},j,k+1}}{\Delta x} \tag{10}$$

$$\frac{\partial}{\partial y}(g.\nabla I_y)\Big|_{i,j,k+1} \approx \frac{g.I_y|_{i,j+\frac{1}{2},k+1} - g.I_y|_{i,j-\frac{1}{2},k+1}}{\Delta y} \tag{11}$$

The derivative for equations (10) and (11) can be obtained by:

$$\begin{aligned} g.I_x|_{i+\frac{1}{2},j,k+1} &\approx g_{i+\frac{1}{2},j,k+1}\left(\frac{I_{i+1,j,k+1} - I_{i,j,k+1}}{\Delta x}\right) \\ g.I_x|_{i-\frac{1}{2},j,k+1} &\approx g_{i-\frac{1}{2},j,k+1}\left(\frac{I_{i,j,k+1} - I_{i-1,j,k+1}}{\Delta x}\right) \\ g.I_y|_{i,j+\frac{1}{2},k+1} &\approx g_{i,j+\frac{1}{2},k}\left(\frac{I_{i,j+1,k+1} - I_{i,j,k+1}}{\Delta y}\right) \\ g.I_y|_{i,j-\frac{1}{2},k+1} &\approx g_{i,j+\frac{1}{2},k+1}\left(\frac{I_{i,j,k+1} - I_{i,j-1,k+1}}{\Delta y}\right) \end{aligned} \tag{12}$$

substituted the equations (8), (9), (10), (11) and (12) into equation (7), then forming the equation as follows:

$$\frac{I_{i,j,k+1}-I_{i,j,k}}{\Delta t} \cong \frac{g_{i+\frac{1}{2},j,k+1}\left(\frac{I_{i+1,j,k+1}-I_{i,j,k+1}}{\Delta x}\right)-g_{i-\frac{1}{2},j,k+1}\left(\frac{I_{i,j,k+1}-I_{i-1,j,k+1}}{\Delta x}\right)}{\Delta x}+\frac{g_{i,j+\frac{1}{2},k+1}\left(\frac{I_{i,j+1,k+1}-I_{i,j,k+1}}{\Delta y}\right)-g_{i,j+\frac{1}{2},k+1}\left(\frac{I_{i,j,k+1}-I_{i,j-1,k+1}}{\Delta y}\right)}{\Delta y} \quad (13)$$

where $h=\Delta x=\Delta y,\ \lambda=\frac{\Delta t}{h^2}$. Thus the approximate equation and be written as follows:

$$I_{i,j,k+1}-\lambda\left[G_N\left(I_{i,j+1,k+1}-I_{i,j,k+1}\right)+G_S\left(I_{i,j-1,k+1}-I_{i,j,k+1}\right)+G_E\left(I_{i+1,j,k+1}-I_{i,j,k+1}\right)+G_W\left(I_{i-1,j,k+1}-I_{i,j,k+1}\right)\right]\cong I_{i,j,k} \quad (14)$$

by rearranging the equation (14) we can finalize the approximate equation as shown below:

$$(1+\lambda G_N+\lambda G_S+\lambda G_E+\lambda G_W)I_{i,j,k+1}-\lambda G_N I_{i,j+1,k+1}-\lambda G_S I_{i,j-1,k+1}-\lambda G_E I_{i+1,j,k+1}-\lambda G_W I_{i-1,j,k+1}\cong I_{i,j,k} \quad (15)$$

where $\lambda>0$. This discretization scheme forms a computation molecule of 4 nearest neighbours of the Laplacian operator as illustrated in Figure 1. Symbols of N, S, E, W indicates the difference between the nearest-neighbour while G_N, G_S, G_E and G_W refer to diffusivity coefficient that is updated at every iteration:

$$G_{N\,i,j,k+1}=g\left(\left\|\nabla I_{i,j+\frac{1}{2},k+1}\right\|\right)$$
$$G_{S\,i,j,k+1}=g\left(\left\|\nabla I_{i,j-\frac{1}{2},k+1}\right\|\right)$$
$$G_{E\,i,j,k+1}=g\left(\left\|\nabla I_{i+\frac{1}{2},j,k+1}\right\|\right)$$
$$G_{W\,i,j,k+1}=g\left(\left\|\nabla I_{i-\frac{1}{2},j,k+1}\right\|\right). \quad (16)$$

The approximation equation for the norm of gradient in (16) can be estimated with absolute value of its projection along the direction of arc shown as:

$$G_{N\,i,j,k+1}=g\left(\left|I_{i,j+1,k+1}-I_{i,j,k+1}\right|\right)$$
$$G_{S\,i,j,k+1}=g\left(\left|I_{i,j-1,k+1}-I_{i,j,k+1}\right|\right)$$
$$G_{E\,i,j,k+1}=g\left(\left|I_{i+1,j,k+1}-I_{i,j,k+1}\right|\right)$$
$$G_{W\,i,j,k+1}=g\left(\left|I_{i-1,j,k+1}-I_{i,j,k+1}\right|\right). \quad (17)$$

The approximation of equation (15) produce $(M-1)^2$ equation based on the number of pixels for the tested image. Lastly, the equations will be solved by the iterative method such as Jacobi, Gauss-Seidel and SOR.

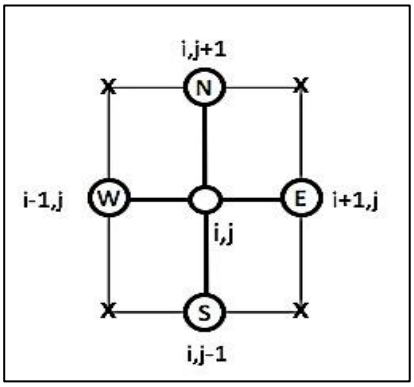

Figure 1. Computational molecule of implicit scheme of equation (15)

3.2 Formulation of SOR Iterative Method

The anisotropic diffusion equation for image blurring is solved by using three iterative methods: Jacobi, Gauss-Seidel and SOR. The matrices form by a stack of linear equation from approximation equation (18) was developed to simplify the formulation of the iterative process. Consider the matrix form of the system of linear equation for solution image blurring as shown in the following:

$$A\underline{I}=\underline{b} \quad (18)$$

where Matrix A is the main diagonal which has no zeroes coefficient. Matrix A also can be split into three different matrices:

$$A\,A=D-F-G. \quad (19)$$

Matrices D, F and G refer to the diagonal, strict lower triangular and strict upper triangular parts of matrix A, respectively. Then equation (19) is merged into equation (18) to form:

$$(D-F-G)I=b. \quad (20)$$

Thus, Jacobi iterative method to solve the linear system can be written in matrix-vector notation as:

$$I^{(k)}=D^{-1}(F+G)I^{(k-1)}+D^{-1}b. \quad (21)$$

The Gauss-Seidel method can be written as:

$$I^{(k)}=(D-F)^{-1}GI^{(k-1)}+(D-F)^{-1}b \quad (22)$$

for $k=1,2,3,\dots,n$.

Successive Over-Relaxation (SOR) iterative method is actually a modification of the Gauss-Seidel iterative method. The only difference in the SOR method is adding ω as a relaxation parameter. By rearranging equation (19) as shown in Gauss-Seidel and adding the parameter ω which has been introduced by Young in 1955, we get [10]:

$$(D-\omega F)I^{(k)}=[\omega G+(1-\omega)D]I^{(k-1)}+\omega b. \quad (23)$$

where $k=1,2,3,\dots,n$. The SOR iterative method can be written in matrix-vector notation as follows:

$$I^{(k)}=(D-\omega F)^{-1}[\omega G+(1-\omega)D]I^{(k-1)}+\omega(D-\omega F)^{-1}b. \quad (24)$$

with $k=1,2,3,\dots,n$. By applying the three methods from equations (21), (22) and (24) into equation (15), the corresponding iteration scheme for Jacobi, Gauss-Seidel and SOR are given as follows:

$$I_{i,j}^{(k+1)}\cong\frac{I_{i,j}^{(k)}+\lambda G_N I_{i,j+1}^{(k)}+\lambda G_S I_{i,j-1}^{(k)}+\lambda G_E I_{i+1,j}^{(k)}+\lambda G_W I_{i-1,j}^{(k)}}{1+\lambda G_N+\lambda G_S+\lambda G_E+\lambda G_W}, \quad (25)$$

$$I_{i,j}^{(k+1)}\cong\frac{I_{i,j}^{(k)}+\lambda G_N I_{i,j+1}^{(k)}+\lambda G_S I_{i,j-1}^{(k+1)}+\lambda G_E I_{i+1,j}^{(k)}+\lambda G_W I_{i-1,j}^{(k+1)}}{1+\lambda G_N+\lambda G_S+\lambda G_E+\lambda G_W}, \quad (26)$$

and

$$I_{i,j}^{(k+1)}\cong\omega\left(\frac{I_{i,j}^{(k)}+\lambda G_N I_{i,j+1}^{(k)}+\lambda G_S I_{i,j-1}^{(k)}+\lambda G_E I_{i+1,j}^{(k)}+\lambda G_W I_{i-1,j}^{(k)}}{1+\lambda G_N+\lambda G_S+\lambda G_E+\lambda G_W}\right)+(1-\omega)I_{i,j}^{(k)} \quad (27)$$

for $k=1,2,3,\dots,n$.

4. Results and Discussion

In this work, we considered three examples of color image as shown in Figure 2 of different sizes or resolutions. The iterative methods were applied to each input image and the number of iterations and computational time for the image to blur were recorded. We employed Jacobi iterative as the control method with iteration parameter $k=100$ and $k=500$ iterations, and threshold parameter, $K=2$. The iterations for Gauss Seidel and SOR were stopped when the quality of the output image of both methods were the same with image

produced by the Jacobi, where overall pixel difference between Gauss-Seidel or SOR and Jacobi images is less than 1%.

(a)

(b)

(c)

Figure 2. (a), (b) and (c) show the input images

Since the algorithm filtered colour image, the iterations are running three times for each colour (Red, Green and Blue) channels separately causing each colour recorded different number of iterations k and computational time t. The average number of iterations k and computational time t of the three channels run for each image are recorded in Tables 1 and 2. For Jacobi method, two different values are used for the control parameter $k = 100$ and $k = 500$.

In Table 1, the control parameter k for Jacobi is set to 100. It can be seen that both Gauss-Seidel and SOR required less iterations k and faster computation time t compared to Jacobi. The number of iterations k for Gauss-Seidel and SOR had been reduced approximately by 23%-34% and 67%-76% respectively. It can also be observed that the computational time t taken by Gauss-Seidel and SOR against Jacobi are reduced approximately by 17%-39% and 65%-69%, respectively. There is no significant difference in terms of the quality of the final output images produced by all three methods as illustrated in Figure 3.

(a)

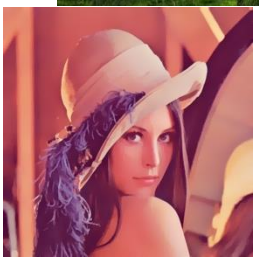

$k = 100$

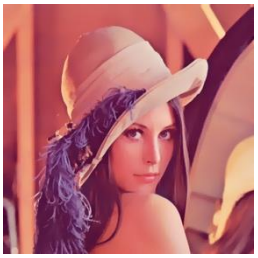

$k = 66$

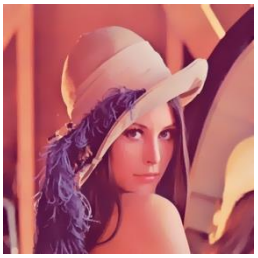

$k = 25$

(b)

$k = 100$

$k = 65$

$k = 24$

(c)

$k = 100$

(i)

$k = 77$

(ii)

$k = 33$

(iii)

Figure 3. The output image produced by (i) Jacobi at $k = 100$, (ii) Gauss-Seidel and (iii) SOR iterative methods

Table 1. The number of iterations *k* and computational time *t* (in milliseconds) for image blurring by Jacobi, Gauss-Seidel and SOR methods. For Jacobi, the control parameter *k* is set to 100

Resolution/ Method	**Jacobi**		**Gauss-Seidel**		**SOR**	
	k	***t***	***k***	***t***	***k***	***t***
(a)512x512	100	6325	66	4899	25	2215
(b)1280x834	100	45386	65	27746	24	14080
(c)1920x1267	100	126023	77	105004	33	43095

Table 2 shows the results of image blurring for the three methods with control parameter *k* for Jacobi is set to 500. The reduction of percentage in terms of *k* and *t* as shown in Table 2 is similar to Table 1. Against the control Jacobi method, the SOR had successfully reduced their number of iterations *k* and computational time *t* approximately by 63%-77% and 54%-80%, respectively. Again, there is no noticeable difference in terms of quality of the final output images produced by the three iterative methods, as shown in Figure 4.

Figure 4. The output image produced by (i) Jacobi at $k = 500$, (ii) Gauss-Seidel and (iii) SOR iterative methods

Table 2. The number of iterations *k* and computational time *t* (in milliseconds) for image blurring by Jacobi, Gauss-Seidel and SOR methods. For Jacobi, the control parameter *k* is set to 500

Resolution/Method	**Jacobi**		**Gauss-Seidel**		**SOR**	
	k	***t***	***k***	***t***	***k***	***t***
(a)512x512	500	29575	397	27388	183	13431
(b)1280x834	500	243628	394	173350	113	45690
(c)1920x1267	500	677311	425	535510	171	237568

5. Conclusion

Three iterative methods, i.e. Jacobi, Gauss-Seidel and SOR were examined to compute the solutions of anisotropic diffusion equation for application in image blurring. The Jacobi was used as a control method with fixed iterations, $k = 100$ and $k = 500$. As expected, the results show that the SOR iterative method is superior to Jacobi and Gauss-Seidel with the least number of iterations and computational time in producing the same quality of Jacobi image. As shown in Figures 3 and 4, there is no significant difference in terms of quality of the final images. Apart from the SOR iterative method which is categorized as a family of one parameter iterative method, further study should be made to investigate the efficiency of the two parameters of relaxation methods such as MSOR [22] and HSAOR [23]. In this research all example pictures used from standard source [24].

References

[1] G. Aubert, P. Kornprobst, *Mathematical Problems in Image Processing: Partial Differential Equations and the Calculus of Variations*. Springer-Verlag, New York, 2002.

[2] W. Zhang, J. Li, Y. Yang, "A fractional diffusion-wave equation with nonlocal regularization for image denoising", *Signal Processing*, vol. 103, pp. 6-15, 2014.

[3] R. Brancaccio, M. Bettuzzi, M. P. Morigi, F. Casali, G. Levi, G. Baldazzi, P.Inferrera, "Preliminary results of a new approach for three-dimensional reconstruction of Dynamic AngioThermography (DATG) images based on theinversion of heat equation", *European Journal of Medical Physics*, vol. 32, no. 9, pp. 1052-1064, 2016.

[4] R. Maeda, T. Maruyama, "An implementation method of Poisson Image Editing on FPGA", in *27th International Conf. on Field Programmable Logic and Applications (FPL)*, Ghent, pp. 1-6, 2017.

[5] W. He, W. Ye, L. Ping, M. Yining, "The PDE method of image segmentation", in *2012 Symposium on Photonics and Optoelectronics (SOPO)*, Shanghai, pp. 1-3, 2012.

[6] H. K. Rafsanjani, M. H. Sedaaghi, S. Saryazdi, "An adaptive diffusion coefficient selection for image denoising", *Digital Signal Processing*, vol. 64, pp. 71-82, 2017.

[7] J. Xu, Y. Jia, Z. Shi, K. Pang, "An improved anisotropic diffusion filter with semi-adaptive threshold for edge preservation", *Signal Processing*, vol. 119, pp. 80-91, 2016.

[8] J. Weickert, *Anisotropic diffusion in image processing*, Stuttgart, Teubner, 1998.

[9] J. Weickert, S. Ishikawa, A. Imiya, "Linear scale-space has first been proposed in Japan", *Journal of Mathematics Imaging and Vision*, vol. 10, no. 3, pp. 237-242, 1999.

[10] E. J. Hong, A. Saudi, J. Sulaiman, "Application of SOR Iteration for PoissonImage Blending", in *Proceedings of the International Conference on High Performance Compilation, Computing and Communications*, Kuala Lumpur, pp. 60-64, 2017.

[11] E. Yilmaz, T. Kayikcioglu, S. Kayipmaz, "Noise removal of CBCT image usingan adaptive anisotropic diffusion filter", in *40th International Conference on Telecommunications and Signal Processing (TSP)*, pp. 650-653, 2017.

[12] W. Wu, C. Zhong, "An Improved Nonlinear Diffusion Algorithm forImage Denoising", in *International Conference on Computer, Mechatronics, Control and Electronic Engineering (CMCE)*, pp. 188-191, 2010.

[13] F. Karami, L. Ziad, K. Sadik, "A splitting algorithm for a novel regularization of Perona-Malik and application to image restoration", *EURASIP Journal on Advances in Signal Processing*, vol. 46, pp. 1-9, 2017.

[14] A. Atlas, F. Karami, D. Meskine, "The Perona–Malik inequality and applicationto image denoising", *Nonlinear Analysis: Real World Applications*, vol. 18, pp. 57-68, 2014.

[15] X. Yu, C. Wu, T. Jia, S. Chen, "A time-dependent anisotropic diffusion image smoothing Method", in *2nd International Conference on Intelligent Control and Information Processing (ICICIP)*, pp. 859-862, 2011.

[16] P. Perona, J. Malik, "Scale-space and edge detection using anisotropic diffusion", *IEEE Transactions on Pattern Analysis and Machine Intelligence*, vol. 12, no. 7, pp. 629-639, 1990.

[17] F. Catte, P. L. Lions, J. M. Morel, T. Coll, "Image selective smoothing andedge detection by nonlinear diffusion", *SIAM Journal On Numerical Analysis*, vol. 29, no. 2, pp. 182-193, 1992.

[18] A. H. Fredj, J. Malek, E. B. Bourennane, "Fast oriented anisotropic diffusion filter", in *11th International Design & Test Symposium (IDT)*, Hammamet, pp. 308-312, 2016.

[19] K. Krissian, C. F. Westin, R. Kikinis, K. G. Vosburgh, "Oriented speckle reducing anisotropic diffusion", *IEEE Transactions on Image Processing*, vol. 16, no. 5, pp. 1412-1424, 2007.

[20] S. A. Bakalexis, Y. S. Boutalis, B. G. Mertzios, "Edge detection and image segmentation based on nonlinear anisotropic diffusion", in *14th International Conference on Digital Signal Processing Proceedings*, vol. 2, pp. 1203-1206, 2002.

[21] R. Ahmmed, M. F. Hossain, "Tumor Detection in Brain MRI image using template based K-means and Fuzzy C-means clustering algorithm", in *International Conference on Computer Communication and Informatics (ICCCI)*, pp. 1-6, 2016.

[22] E. J. Hong, A. Saudi, J. Sulaiman, J. "Numerical assessment for poisson image blending problem using MSOR iteration via five-point laplacian operator", *Journal of Physics: Conference Series*, vol. 890, 2017.

[23] E. J. Hong, A. Saudi, J. Sulaiman, "HSAOR iteration for poisson image blending via rotated five-point laplacian operator", *Global Journal of Pure and Applied Mathematics*, vol. 12, no. 9, pp. 5447-5459, 2017.

[24] Test examples obtained from https://pixabay.com/